Proceedings of ICFDP9:
Ninth International Congress of Fluid Dynamics & Propulsion
December 18-21, 2008, Alexandria, Egypt

ICFDP9-EG-285

EFFECT OF END STEP ON FLOW CHARACTERISTICS DOWNSTREAM OF RADIAL GATES IN STILLING BASIN OF NAGA HAMMADI BARRAGE PHYSICAL MODEL

Abdelazim M. Ali
Hydraulics Research Institute, National Water Research Center, MWRI, Egyp
abdelazim@hri-egypt.org

Aabdelazim M. Negm
Water and Water Structures Eng. Dept., Faculty of Eng., Zagazig University, Zagazig,
amnegm85@yahoo.com

Mohamed H. El Gamal
Hydraulics and Irrigation Dept., Faculty of Eng., Cairo Uiversity, Cairo, Egypt.

Mohamed F. Helwa
Hydraulics and Irrigation Dept., Faculty of Eng., Cairo Uiversity, Cairo, Egypt.

Mohamed B. Saad
First under Secretary of the Ministry, MWRI, Egypt

ABSTRACT

In this paper, effect of positive step located at the end of the stilling basin (called end step) on the flow characteristics downstream the radial gate of the New Naga Hammadi Barrages physical model were investigated. These characteristics include the main parameters of the submerged hydraulic jump, the vertical velocity distribution along the bed, the velocity decay, and the stability of bed protection downstream the apron of the stilling basin. Three different heights of the end step were tested. The physical model was built at the Hydraulics Research Institute, Delta Barrage, Egypt. The used flume has 1.0 m wide, 26.0 m long and 1.20 m deep. The flume side walls are made of glass with steel-frames to allow visual investigation of the flow patterns and stability of bed protection.

The analysis and discussion of results indicated that the best relative height of the end step is about 0.14. This relative height provides the shortest length of submerged hydraulic jump, faster decay of near bed velocity, shortest length from the gate to the section where the velocity distribution is fully developed, minimum scour dimensions DS of basin and hence highest stability of bed protection.

KEYWORDS:

Stilling basin, flow characteristics, hydraulic jump, velocity distribution, bed protection, scour, end step.

INTRODUCTION

Old and new barrages have been built on the Nile River in order to regulate water distribution and control flows to maximize profitability and minimize losses, such as Assuit, Esna, and Naga Hammadi Barrages by the Ministry of Water Resources and Irrigation (MWRI). During the testing of New Esna Barrage design and performance on a physical model, it was observed that the scour immediately downstream the stilling basin exceeded the expected values. This observation has been verified further during the monitoring of the actual structure. The same findings were also observed during the design and model testing of New Naga Hammadi Barrage. In both cases significant design modifications has been introduced using trail and error based on expert's opinion. Therefore, there is a need to develop and improve some design criteria for hydraulic structures to be used in future applications and suitable for the Nile River conditions [4].

Previous investigations on submerged hydraulic jumps and stilling basins are numerous, e.g. [1,8,9,10,19]. Also, many studies were interested in the investigation of scour and its control downstream of the hydraulic structures and specially stilling basins, e.g. [2,7,11,12,13,15,16,20,21]. Moreover, few studies involved measurements of velocity near bed during the different operations of multi-vents barrages [14,16]. Some studies investigates the effect of using under-gate sill on free flow downstream gates, e.g. [17,18] and others on submerged flow downstream gates, e.g. [5,6,18] However, none of all these studies was conducted on a barrage physical model that represents the Nile river conditions. Only, Ali et al. [4] investigated the effect of under-gate sill on the length of the submerged jump, the velocity and scour patter and velocity decay using a physical model for Naga Hammadi. It was found that the stilling basin with flat bed is the best selection among the tested set. It was felt that the end step n the stilling basin improves the performance of the basin, therefore the important flow characteristics are investigated under the effect of different heights of the end step.

THEORETICAL BACKGROUND

Figure 1 depicts the definition sketch for the submerged flow downstream of a radial gate with sill under the gate. Using the dimensional analysis, the following functional relationship was obtained between the relative length of the submerged

hydraulic jump, Lsj/y1, (y1 is the depth at the vena contracta) and the other controlling variables.

$$\frac{Lsj}{y_1} = f\left(\frac{K1}{Hu}, \frac{h}{H_u}, \frac{y_t}{y_1}, F_{r1}\right) \quad (1)$$

in which k1/Hu is the relative height of end step, h/Hu is the relative differential head, yt/y1 is the relative tail water depth or submergence and Fr1 is the Froude number at the vena contracta. All tests were conducted under particular tailwater conditions. Therefore, yt/y1 is of minor importance due to the fact of being keeping it invariable.

Similarly, the relationship between the relative near bed velocity, vb/v1, (v1 is the velocity at the vena contracta) and the controlling variables could be obtained as follow.

$$\frac{v_b}{v_1} = f\left(X, \frac{k1}{Hu}, \frac{h}{H_u}, \frac{y_t}{y_1}, F_{r1}\right) \quad (2)$$

Where X is the relative horizontal distance where the velocity is measured. The other symbols used in equations (1) and (2) are defined in both Figure 1 and in the nomenclatures section at the end of the paper.

It should be noted that similar equations may be written for the relative maximum depth of scour, the relative tailwater depth of the submerged hydraulic jump and the relative energy loss of the submerged hydraulic jump.

PHYSICAL MODEL AND EXPERIMENTATION

The experiments were conducted using a 1.0 m wide, 26.0 m long and 1.20 m deep flume. The side walls along the entire length of the flume are made of glass with steel-frames, to allow visual investigation of the flow patterns and stability of bed protection. The horizontal bottom of the flume is made of concrete and provided with a steel pipe to drain the water from the flume. The tail water depth is controlled by a tailgate located at the downstream end of the flume. The water enters the flume from a constant head tank, which is fed by a centrifugal pump with a maximum discharge of 0.5 m^3/s (500 l/s) through an 16 inches pipeline. The flume is provided with another pump of capacity 150 l/s through an 10 inches pipeline to increase the discharge whenever required. A recirculating discharge system was used and there was underground reservoir of a total capacity of 80 m^3. An ultrasonic flowmeter was installed on the feeder pipe of 10 inches diameter and an electro-magnetic flowmeter was installed on the feeder pipe of 16 inches diameter. These two flowmeters are used for measuring the discharge during the tests with accuracy of ± 1%. A currentmeter for measuring the flow velocity was used. A data logger for collecting the data and transferred it to the computer was used. Point gauges for adjusting the water level at both upstream and downstream the gate and measuring the scour hole were used. A digital camera for recording the scour downstream the apron was employed. All equipments and instrumentations which needs calibration were calibrated at HRI before and during carrying out the model work. All equipments performance and accuracy were checked weekly.

The flume inlet consists of a masonry basin of 3.0 m width, 3.0 m length and 2.5 m depth. This entrance receives the delivered water from the pump through a pipeline to dissipate the energy of the flow that enters the model and to avoid any disturbance of the flow in the flume. A weir was built at the entrance. The water passes through a screen box filled with large gravel followed by another screen box filled with 2 inch-diameter plastic pipes to dissipate the energy at the inlet to suppress any excessive turbulence.

A bras radial gate with a radius of 52.4cm was used to regulate the flow. The gate opening was measured by using a vertical scale. A rubber strip was fixed at both sides to be compressed to the flume sides when the gate slides. This arrangement ensured no leakage from the flume sides. The test model was fixed to the flume bed under the gate and extended from both sides DS and US of the gate. A sill is provided under he radial gate as shown in Figure 1. An end step was constructed at the end of the basin. Three different heights of the step was tested, viz k1=0.09 m, 0.06 m and 0.03 m.. The rigid bed is followed by a 3m long movable bed covered by rip rap with d_{50}=1.5cm. The upstream and the downstream parts of the radial gate are considered a part of the physical model, which was filled, with sand of 0.51 mm mean diameter. The upstream part was shaped in such way to enhance the flow and make it smooth when it approaches the gate. Also, the downstream part of the model was shaped to distribute the flow uniformly. The movable bed, at the downstream part, comprises of three different layers, sand, filter, and riprap with the properties shown in table 1 and Figure 1

LIMITATIONS OF HYDRAULIC VARIABLES

The hydraulic variables were designed in such a way to cover a wide range of barrages along the Nile River such as New Esna Barrage, New Naga Hammadi Barrage, Assuit Barrage, Delta Barrage, Zifta and Idfina Barrages. The main hydraulic variables were; the discharge, Q (ranges from 5 to 25 m3/s/m), differential head, h (ranges from 3-8 m) and the downstream water depth, yt (ranges from 6.5 to 12.5 m). These ranges of the hydraulic variables were based on the prototype hydraulic conditions of the different barrages on the Nile River. The hydraulic conditions for all test series were prepared based on the prototype hydraulic conditions. In the models the upstream head was kept constant, the discharge ranges from 40 to 190 lit/s, the downstream head varies from 0.47 to 0.64 m while the differential head varies from 0.16 to 0.33 m. For more details, one may consults Ali [3].

Table 1: Properties of bed protection materials

Material Characteristics	Sand	Filter	Rip Rap
D15 (mm)	0.36	3.60	11.80
D50 (mm)	0.49	4.70	15.54
D85 (mm)	0.67	6.10	18.50
D84/D50	1.35	1.29	1.19
D50/D16	1.34	1.27	1.31

MODEL TEST PROCEDURES

The following systematic steps were followed to carry out any particular run of the three tested models. Each model was tested under six flow conditions, and each flow conditions have six tailwater depths i.e., 36 conditions for each model. The following procedure was used to conduct these tests [3,4].

1. The level of the bed protection downstream the apron was adjusted at the same level as the apron.
2. The underground tank was filled with clear water.
3. The pump was operated and the flow was adjusted by the control valve and measured by an electromagnetic flowmeter or ultrasonic flowmeter.
4. The upstream and downstream water depths were adjusted to the required test condition.
5. After reaching the stability the following measurements were recorded, the gate opening (a), the back up water depth (y_3), the initial water depth of the jump (y_1), the length of jump (L_{sj}), the velocity profiles at seven cross sections and the velocity near bed at 3 cm from the bed level.
6. The bed protection downstream the apron was reshaped.
7. The tailwater depth was changed and steps no. 5 and 6 were repeated for six tailwater depth condition.
8. The discharge was changed and steps 5, 6, 7 and 8 were repeated.
9. The test procedure was repeated for each of the three tested end step models.

THE UNDERTAKEN MEASUREMENTS

During each test, the flow velocity was measured at seven cross sections distributed along the centerline of the simulated bay. Also, the scour of the protected bed, downstream the apron, was measured. The submerged hydraulic jump characteristics were measured. The scour of the bed, downstream the apron and the jet under the radial gate, was recorded by the digital camera. Regarding, the flow velocity measurements were measured using an electromagnetic current-meter type EMS, manufactured by Delft Hydraulics, Holland. The current-meter was connected to a data logger, which receives the data directly from the currentmeter. The data logger also was connected to the computer, which receives the data from the data logger and save it in a file. The data logger was set to record 25 readings during time of 10 seconds at each point depth of the cross section. The currentmeter measured the flow velocity in two directions; in the flow direction, and perpendicular to the main flow.

The flow velocity was measured at seven cross sections with equal distances apart. The distance between each two cross section was equal to 0.50m. The first cross section was located at a distance of 1.0m downstream the gate. Four cross sections were located on the apron area, and the other three sections were located on the rip rap area, downstream the apron. Figure 3 shows the location of the velocity profiles. Seven profiles were presented for each test; they are the profiles measured at the different locations downstream the gate. Also, five velocity values were shown on each profile; they are the near bed velocity 3 cm from the bed and the four velocities at 0.2, 0.4, 0.6, and 0.8 relative depth. Each velocity value is actually the average of 25 measurements taken within 10 seconds; also, the velocities shown are the velocities in the main flow direction only. Figures 4 presets a sample of the velocity near bed for the test series with Q=190 lit/s, downstream head =0.63 m and differential head of 0.16 m fo**r** case when no end step is present at the end of the basin.

ANALYSIS OF RESULTS AND DISCUSSIONS

In order to increase the applicability of the results of this investigation, the experimental results were analyzed in dimensionless form. The horizontal measurements, x (distances) were divided by the length of the stilling basin, Lb, to yield the dimensionless parameter X=x/Lb. The relative horizontal distances varies from 0 to 1.6. Both the differential head h and the sill height, e, were divided by the upstream head Hu, to yied h/Hu and e/Hu as obtained from the dimensional analysis. On the other hand, Froude number is dimensionless. Froude number ranges from 1.3 to 2.55. the relative differential head, h/Hu, has the values 0.49, 0.44, 0.38, 0.33, 0.29 and 0.24 on average. The relative height of end step, k1/Hu, has the values of 0.14, 0.10 and 0.05. The velocity profiles at the different locations (X=0.4, 0.6, 0.8, 1.0, 1.2, 1.4 and 1.6) were presented for each e/Hu and each h/Hu values. All these profiles are analyzed and only few typical cases are presented in the paper to reserve space.

VELOCITY DISTRIBUTION AND VELOCITY DECAY

The analysis of all measured velocity profiles under submerged hydraulic jump conditions indicated two parts; main forward flow (lower part) and the backward flow (upper part).

Also, the dimensionless longitudinal velocity distribution reach its typical velocity profile (fully developed flow) at particular relative horizontal distance "X" depending upon the values of "h/Hu", "k1/Hu" and Fr1. Moreover, for a certain value of "h/Hu", "k1/Hu" and "X" the forward flow was increased as the Froude number "Fr1" decreased and the reason for that was due to increasing the gate opening and consequently increasing the thickness of the forward flow. Also, it was observed that by decreasing the "h/Hu" for a certain value of "k/Hu" the thickness of the forward flow increases and travels for long distance with a high velocity and the backward flow was extended in some cases to relative distance "X" equals 1.4 or slightly more. Figures 5 and 6 show typical velocity profiles for h/Hu=0.44 at Fr1=2.26 and for h/Hu=0.33 at Fr1=1.65 respectively for different k1/Hu of 0.14, 0.10 and 0.0.

Comparing between velocity profiles for different k1/Hu at the same Fr1 and constant h/Hu indicates that the forward flow near to bottom was decreased by increasing the relative step height "k1/Hu". Moreover, the dimensionless velocity profile reaches its identical profile in a short distance from the gate by decreasing the relative step height "k1/Hu" for a certain values of "h/Hu" and Fr1.

On the other hand, the dimensionless velocity decay near bed "vb/v1" was plotted for all investigated cases for all values of h/Hu, k1/Hu and Fr1. Typical plots are presented in Figures 7, 8 and 9 for k1/Hu of 0.14, 0.10 and 0.05 respectively at h/Hu=0.44 for different Fr1. It is observed that the values of the velocities near bed along the stilling basin were increased as the Froude number Fr1decreased. Moreover, it was noticed that the velocity near bed reached the end of apron with low values as "k1/Hu" was increased for fixed value of "h/Hu". Figure 10 shows vb/v1 versus X for "h/Hu" equals 0.44, Fr1equals 1.95 and values of "k1/Hu" equals 0.27, 0.14 and 0.0. This figure shows that the case with k1/Hu=0.14 gives better results for the velocity near bed and reaches the end of apron with lower velocity.

LENGTH OF SUBMERGED HYDRAULIC JUMP AND ENERGY LOSS

Figures 11,12 and 13 present the relationship between Ljs/y1 and Fr1 for h/Hu=0.44, 0.33 and 0.24 respectively for different k1/Hu of 0.14, 0.10 and 0.05 as typical plots. These figures and others indicated that the shortest length of the submerged hydraulic jump was obtained when k1/Hu=0.14 for all values of h/Hu and all values of Fr1. Also, the analysis of the dimensionless tailwater depth and the dimensionless energy loss for all cases indicated that the case with k1/Hu=0.14 produces the smallest values of tailwater depths and the maximum energy dissipation compared to all other cases regardless of the value of h/Hu. Figures 14, 15 and 16 present the relationship between the relative energy loss and the Froude number for h/Hu=0.44, 0.33 and 0.24 respectively and different k1/Hu as typical examples. The relationships for the relative tailwater depth are not presented here to reserve space.

SCOUR DOWNSTREAM THE STILLING BASIN

Analysis of all measured scour profiles indicated that the value of the maximum scour depth increases by increasing Froude number, increases by increasing h/Hu and decreases by increasing k1/Hu. Also, the length of the scour profiles has the same trend as the scour depth. Figures 17a and 17b present two typical scour profiles for Fr1=1.45 and 1.6 respectively at h/Hu=0.24 for different k1/Hu of 0.27, 0.14 and 0.0. Also, figures 18a and 18b presents another tow scour profiles for smaller Froude number of 1.12 and 1.27. Inspection of these figures confirmed the above stated findings.

CONCLUSIONS

The analysis and discussions presented in this paper highlighted the following conclusions:

1- The velocity distribution reached its typical shape in a short distance when k1/Hu is 0.14 compared to other values of k1/Hu. The larger the value of k1/Hu, the shorter is the distance traveled by the velocity till it reaches its typical shape, (fully developed velocity profile).
2- The velocity near bed attains its minimum values when k1/Hu equals 0.14 compared to other values of k1/Hu regardless of the values of h/Hu.
3- The velocity near bed is significantly reduced by about 30% to 50% when k1/Hu equals 0.14.
4- The shortest relative length of the submerged hydraulic jump is produced when k1/Hu equals 0.14.
5- The maximum relative energy loss (or maximum energy dissipation) is obtained when k1/Hu equals 0.14.
6- The values of the relative maximum scour depth are minimum when k1/Hu equals 0.14 at e/Hu=0.44 (or k1/Hu=0.10 at e/Hu=0.33 or 0.24). Also, the length of the scour profiles are the shortest ones at the same stated values of k1/Hu and e/Hu.
7- If an end step is used in the stilling basin, it is recommended to use a one with an average value relative height of step of k1/Hu=0.14 due to all the above merits.

NOMENCLATURE

d_{50}	The median particle size of the bed material
e	Distance between sill under gate and the level of apron
e/H_u	Relative distance between sill under gate and the apron
E_1	The specific energy at the beginning of the jump
E_2	The specific energy at the end of the control volume
E_L	The energy dissipated in the jump (E_1-E_2)
F_{r1}	Froude number at vena contracta $(v_1/(gy_1)^{0.5})$
h	The head difference
h/H_u	The relative differential head
F_{r1}	Froude number at vena contracta $(v_1/(gy_1)^{0.5})$
h	The head difference
h/H_u	The relative head difference
L_{k1}	The distance of the end step from the gate

L_p	The length of the pier
L_b	The basin length
L_{sj}	Length of submerged hydraulic jump
Q	The flow rate
d_s	The maximum scour depth
v	Velocity at any point depth of the profile
v_b	Velocity near bed
y_1	The initial water depth of the classical jump
y_t	The tailwater depth at the end of the basin
x	The distance from the radial gate
X	The relative horizontal distance from the gate (=x/L_b)

REFERENCES

[1] G.M. Abdel Alal, "Modeling of Rectangular Submerged Hydraulic Jumps", Alexandria Engineering journal, Vol.43, No.6, pp.865-873, 2004.

[2] N. Abouel-Atta, "Scour Prevention Using a Floor Jets Mechanism" Civil Engineering Research Magazine, Faculty of Engineering, Al-Azhar University. Vol. 17, No. 2, February. pp. 256-268, 1995.

[3] A.M. Ali, "Improving Stilling Basin Designs For The New Barrages on The Nile River", Unpublished Ph.D. Thesis, Cairo University, Faculty Of Engineering, Cairo, Egypt, 2005.

[4] A.M. Ali, A.M. Negm, M.H. El-Gamal, M.F. Helwa, and M.B. Saad, "Investigation of Flow and Scour Characteristics Downstream of Radial Gates of A Barrage Physical Model", Proc. of Riverflow 2008, Turkey, Sep. 3-5, 2008.

[5] A.A. Alhamid, A.M. Negm, G.M. Abdel-Aal and M.A. Matin, "Effect of Taildepth Variation on Submerged Supercritical Flow Below Silled Gates", CERM, Faculty of Engineering, Al-Azhar University, Cairo, Egypt, Jan. 2001 , Vol. 23, No.1, pp.199-220, 2001.

[6] A.A. Alhamid, A.M. Negm, G.M. Abdel-Aal, and M.A. Matin, "Effect of Submergence and Slopes of under-gate sill on discharge characteristics of submerged Subcritical Flow", The Egyptain Journal For Engineering Sciences and Technology, (EJEST Journal), Faculty of Eng., Zagazig University, Zagazig, Egypt, Vol. 6, No.1, Jan., 2002, pp.61-82, 2002.

[7] A.A. El Masry, "Influence Of A Fully Angled Baffled Floor On Scour Behind A Hydraulic Structure" Mansora Engineering Journal, Faculty of Engineering, Mansora University, Vol. 26, No. 4, December. pp.33-44, 2001.

[8] I. El-Azizi, "A Study Of Submerged Hydraulic Jump Stilling Basins Of Low Head Irrigation Structures", M.Sc. Thesis, Faculty of Engineering, Ain Shams University, Egypt, 1985.

[9] N.S. Govinda Rao and N. Rajaratnam, "The Submerged Hydraulic Jump", Journal of Hydraulic Div., Vol.89, No. HY1, pp. 139-163, 1963

[10] W.H. Hager, "Energy Dissipators & Hydraulic Jumps", Kluwer Academic publication, Dordrecht, The Netherlands, pp. 151-173, 1992.

[11] N.M.K. Hassan and R. Narayanan, "Local Scour Downstream Of An Apron" Journal of Hydraulic Engineering, Vol. 111, No. 11, November. pp. 1371-1385, 1986.

[12] M.S. Mohamed, A.M. Negm, and A.A. El-Saiad, "Effect Of Continuous Sill On Scour Downstream Of Hydraulic Structures", Civil Engineering Research Magazine, Faculty of Engineering, Al-Azhar University, Vol. 21, No. 3, July. pp 625-645, 1999.

[13] A.M. Negm, G.M. Abdel-Aal, M.I. Elfiky, and Y.A. Mohmed, "Characteristics Of Submerged Hydraulic Jump In Radial Basins With A Vertical Drop In The Bed", AEJ, Faculty of Eng., Alex. Univ., Egypt, 2002.

[14] A.M. Negm, G.M. Abdelaal, M.M. Elfiky and Y.A Mohamed, "Effects of Multi-Gates Operations on Bottom Velocity Pattern Under Submerged Flow Conditions", Proc. IWTC10 2006, March 23-25, Vol. I, pp.217-280, Alex., Egypt, 2006.

[15] A.M. Negm, "Minimization of Scour DS of Radial Stilling Basin", Proc. Of 11th IWTC2007, 15-18 March 2007, Vol.2, pp.731-740, Sharm Elsheikh, Egyp, 2007.

[16] A.M. Negm, G.M. Abdelaal, M.M. Elfiky, and Y.A. Mohamed, "Effect of Multi-Gates Rgulators Operations on Downstream Scour Pattern Under Submerged Flow Conditions", Proc. IWTC11 2007, March 15-18, Vol. II, pp.735-767, Sharm Elsheikh, Egypt, 2007.

[17] A.M. Negm, M. Abdellateef, and T.M. Owais, "Effect of Under-Gate Sill Crest Shapes on The Supercritical Free Flow Characteristics", Engineering Bulliten, Faculty of Eng., Ain Shams University, Vol.28, No.4, Dec. 1993, Cairo, Egypt, pp.175-186, 1993.

[18] A.M. Negm, "Free and Submerged Flow Below Sluice Gate With Sill", in Advances in Hydroscience and Engineering, Vol.2, Part A, (Ed. CHES and IRTCES), Proceedings of Second ICHE-95, 22-26 March 1995, Tsinghua University Press, Beijing, China, pp. 283-300, 1995.

[19] N. Rajaratnam, "Hydraulic Jump In Advances In Hydro-Science", Vol.14 Edited by V.T. Chow, pp. 197-280, Academic Press, New York and London, 1967.

[20] O.K. Saleh, A.M. Negm, N.G. Ahmed, “Effect Of Asymmetric Side Sill On Scour Characteristics Downstream Of Sudden Expanding Stilling Basins”, Al-Azahr Engineering 7th International Conference. Cairo Egypt, 2003.
[21] A.R. Zidan, T.M. Owais, M. Abdel-Motaim and A. El-Masry, “Scour Behind Sluice Gates” Mansora Engineering Journal, Faculty of Engineering, Mansora University, Vol. 8, No. 2, December. pp.1-19, 1983.

ANNEX A

FIGURES

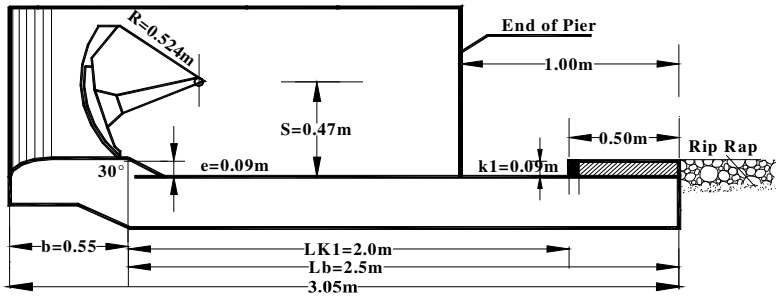

Figure 1. Definition sketch for the test physical model under

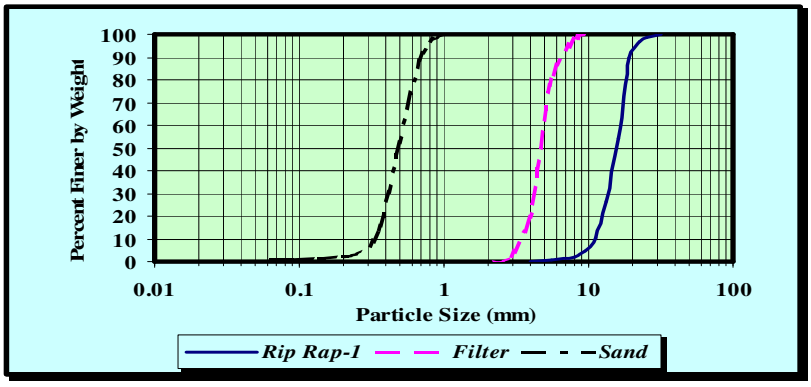

Figure 2. Sieve analysis of sand, filter, and rip rap materials

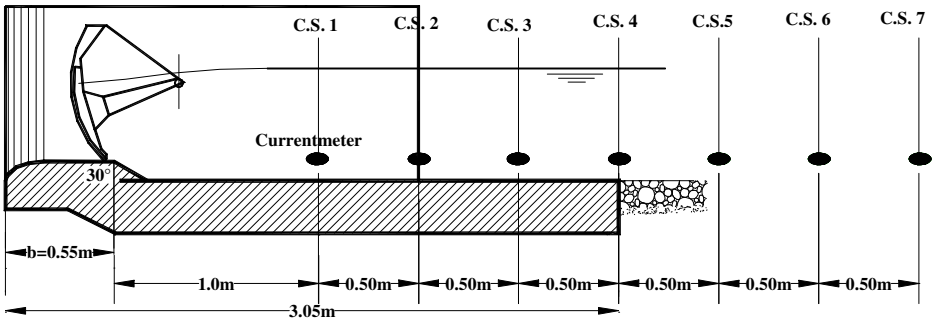

Figure 3. Location of velocity profiles measurements

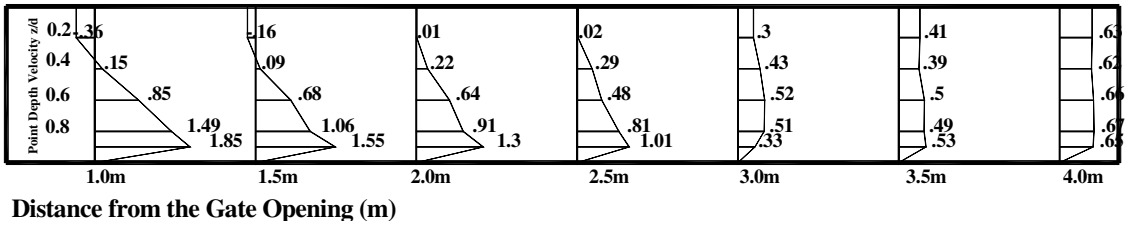

Figure 4. Typical measured velocity profiles at the seven locations for a run with Q= 190 lit/s, downstream head = 0.64 m and differential head of 0.16 m.

.

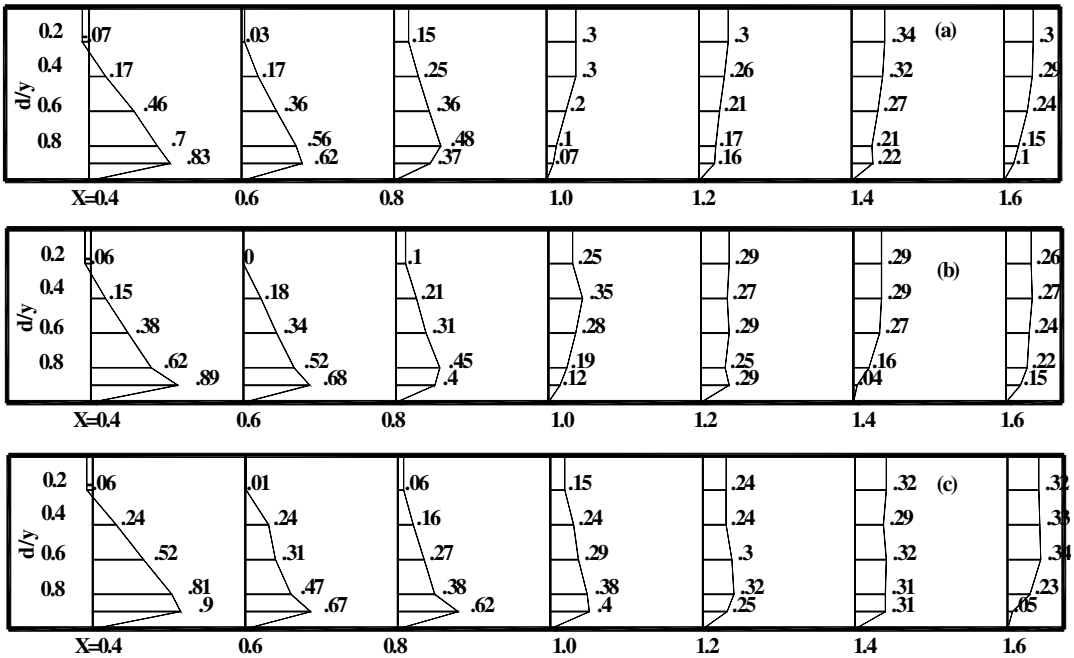

Figure 5. Variation of velocity distribution profiles for h/Hu=0.44 at Fr1=2.26 and k1/Hu= (a) 0.27 (b) 0.14 and (c) 0.0

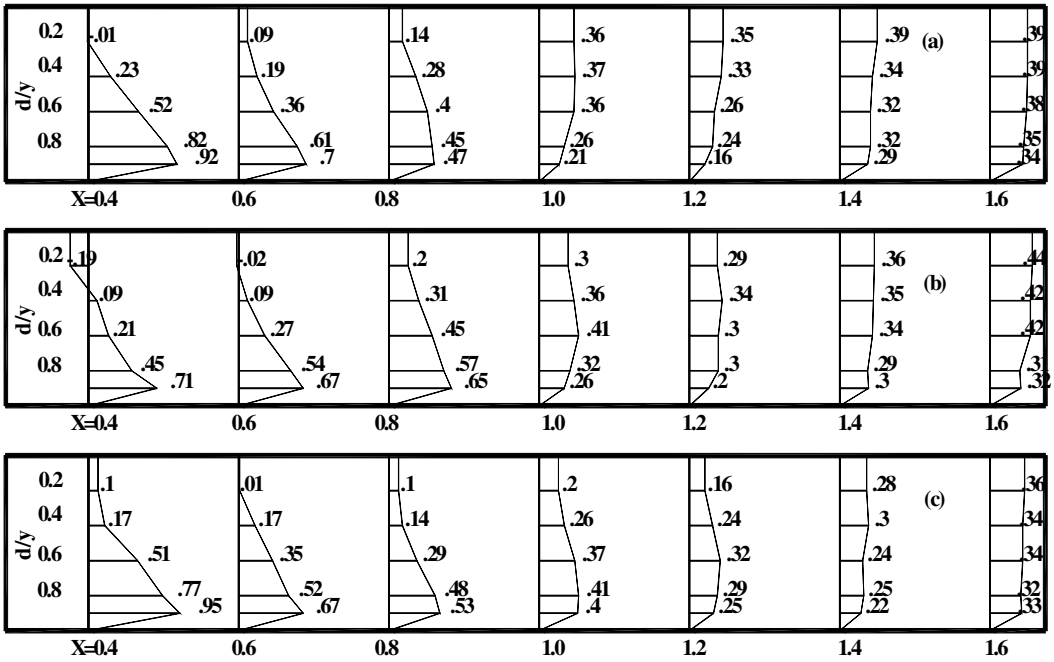

Figure 6 Variation of velocity distribution profiles for h/Hu=0.33 at Fr1=1.95 and k1/Hu= (a) 0.27 (b) 0.14 and (c) 0.0

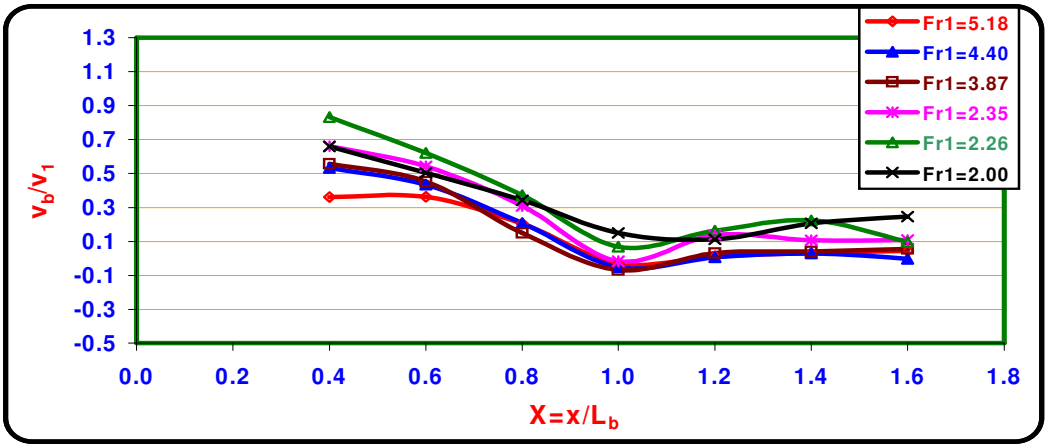

Figure 7. Relationship between vb/v1 and X at h/Hu=0.44, k1/Hu=0.14 and different Fr1

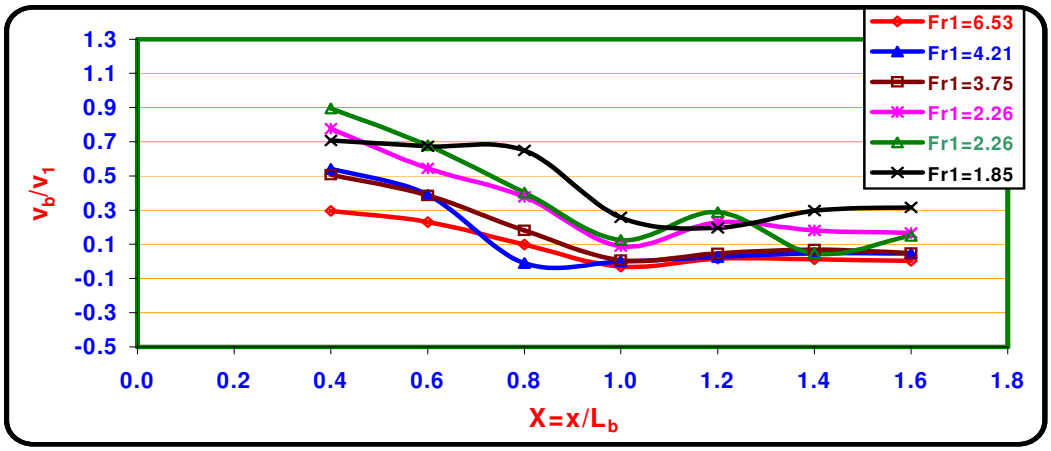

Figure 8. Relationship between vb/v1 and X at h/Hu=0.44, k1/Hu=0.10 and different Fr1

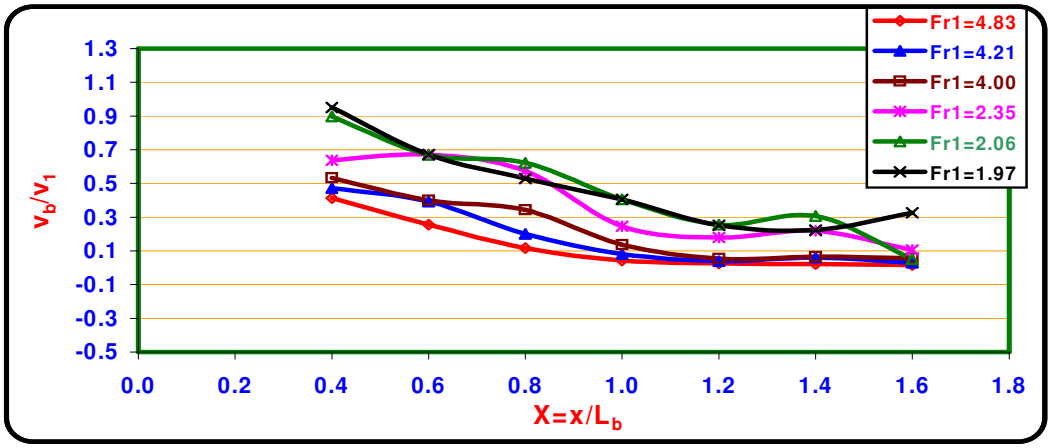

Figure 9. Relationship between vb/v1 and X at h/Hu=0.44, e/Hu=0.05 and different Fr1

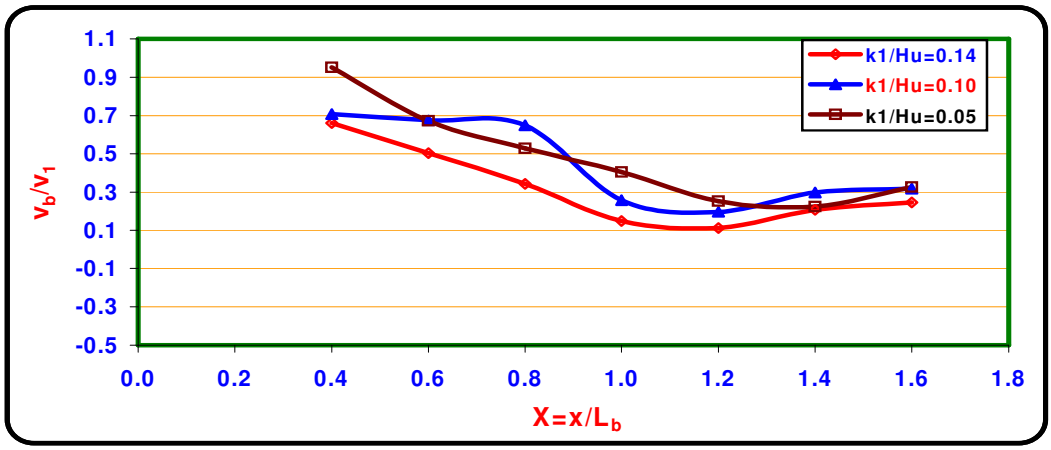

Figure 10. relationship between vb/v1 and X for h/Hu=0.44 and Fr1=1.95 and different k1/Hu of 0.14, 0.10 and 0.05

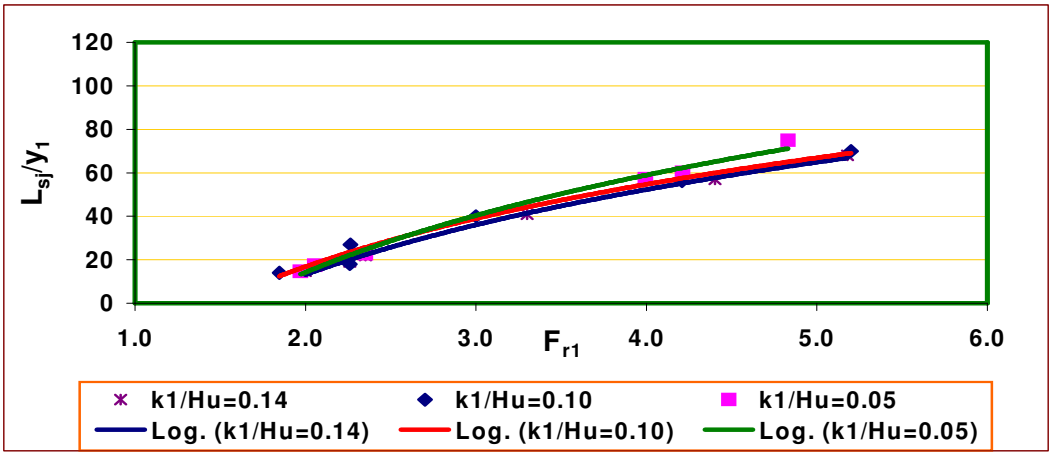

Figure 11. Relationship between Lsj/y1 and Fr1 for h/Hu=0.44 and different k1/Hu

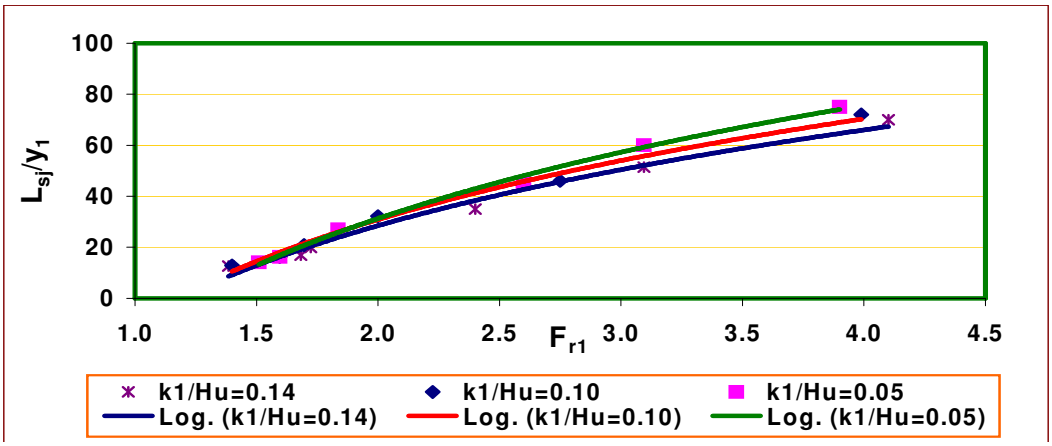

Figure 12. Relationship between Lsj/y1 and Fr1 for h/Hu=0.33 and different k1/Hu

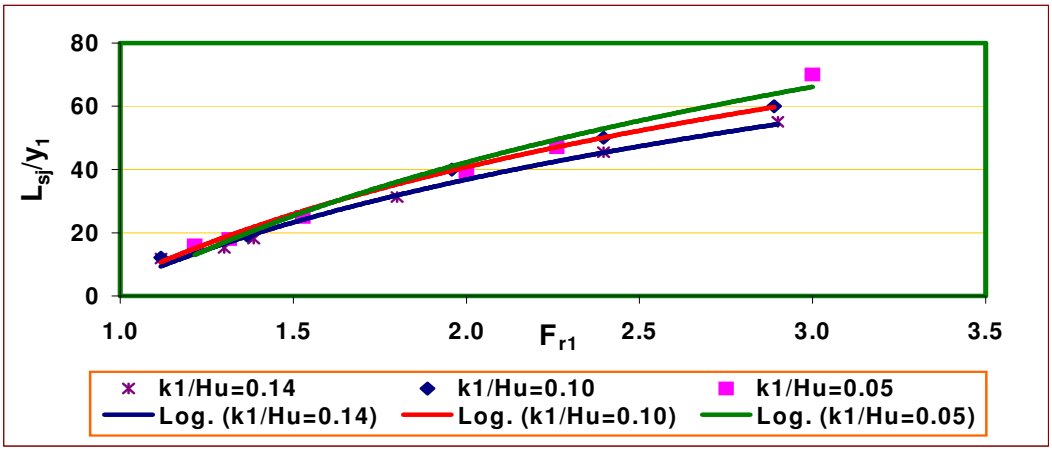

Figure 13. Relationship between Lsj/y1 and Fr1 for h/Hu=0.24 and different k1/Hu

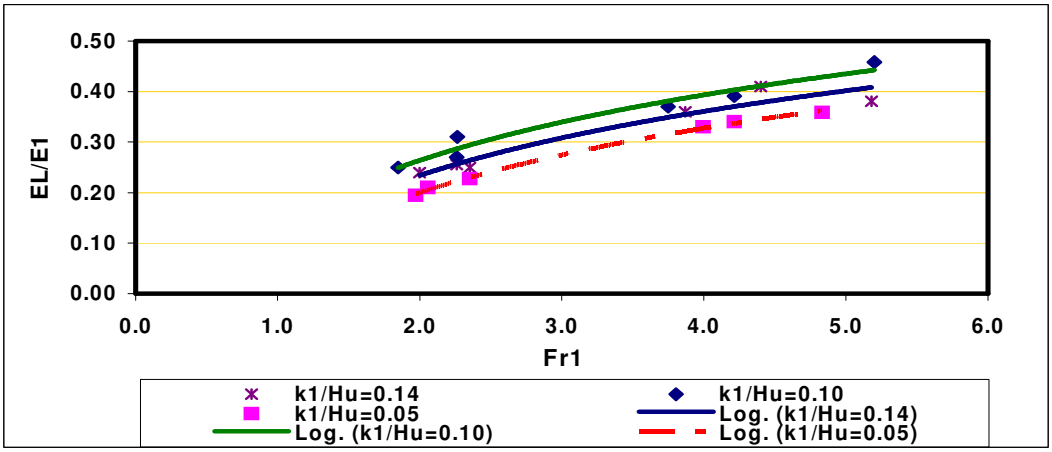

Figure 14. Relationship between EL/E11 and Fr1 for h/Hu=0.44, e/Hu=0.14 and different k1/Hu

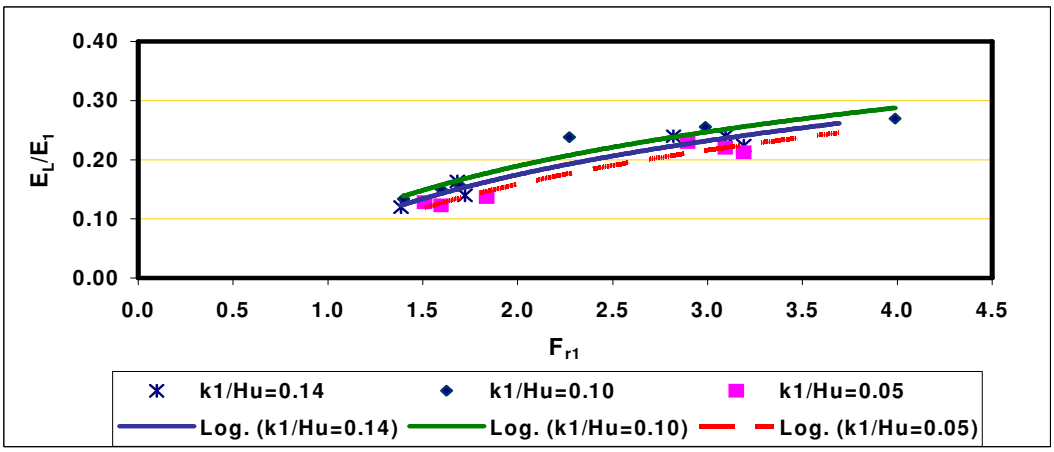

Figure 15. Relationship between EL/E1 and Fr1 for h/Hu=0.33, e/Hu=0.14 and different e/Hu

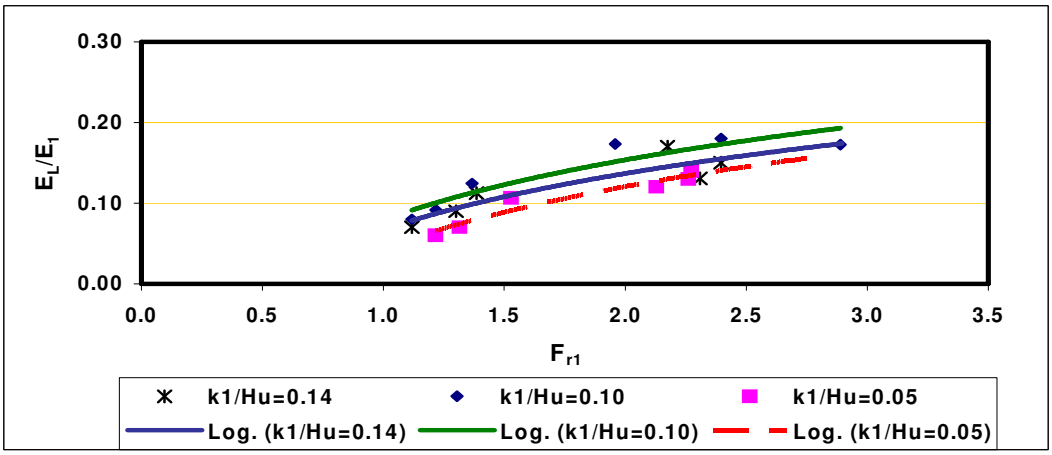

Figure 16. Relationship between EL/E1 and Fr1 for h/Hu=0.24, e/Hu=0.14 and different e/Hu

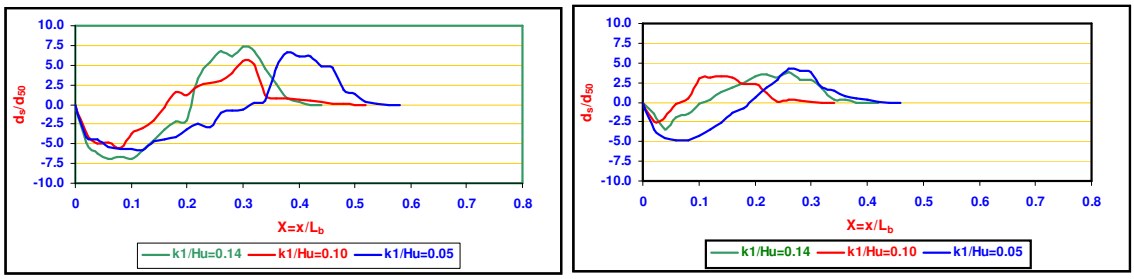

(a) **(b)**

Figure 17 Comparison between the dimensionless scour profile d_s/d_{50} for $k1/H_u$=0.14, 0.10 and 0.05 and h/H_u=0.33 and F_{r1} (a) = 1.45 and (b) = 1.60

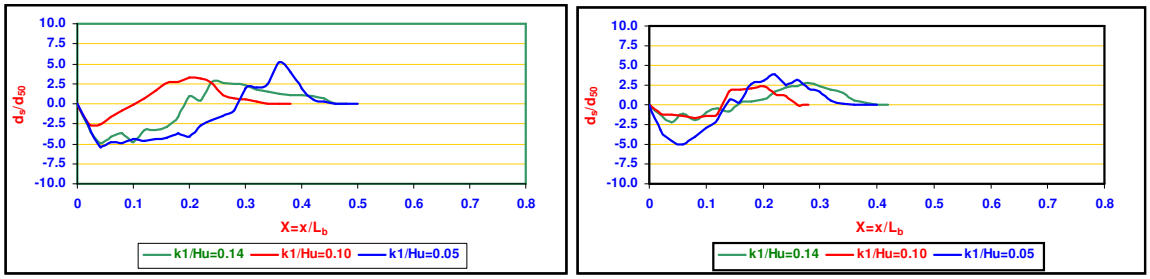

(a) **(b)**

Figure 18 Comparison between the dimensionless scour profile d_s/d_{50} for $k1/H_u$=0.14, 0.10 and 0.05 and h/H_u=0.24 and F_{r1} (a) = 1.12 and (b) = 1.27